EFFECT OF A PRESSURE GRADIENT AND OF EXTERNAL FLOW TURBULENCE ON FLOW IN A BOUNDARY LAYER

G. S. Glushko, V. I. Bronshtein, and B. N. Yudaev

UDC 532.517.4:536.25

The effect of a pressure gradient and of external flow turbulence on the nature of flow in the laminar, transition, and turbulent regions is investigated.

1. The System of Equations

Turbulent flow of an incompressible fluid in a boundary layer is described by a system of equations similar to that suggested by Kolmogorov [3] and investigated in detail by Glushko and Solopov [5-10]. The system consists of the Reynolds, continuity, turbulence energy, turbulence scaling, and heat-transfer equations:

$$u\frac{\partial u}{\partial x}+v\frac{\partial u}{\partial y}=-\frac{1}{\rho}\cdot\frac{\partial p}{\partial x}+\frac{\partial}{\partial y}\left((\nu+\nu_t)\frac{\partial u}{\partial y}\right), \tag{1}$$

$$\frac{\partial u}{\partial x}+\frac{\partial v}{\partial y}=0, \tag{2}$$

$$u\frac{\partial T}{\partial x}+v\frac{\partial T}{\partial y}=\frac{\partial}{\partial y}\left(\left(\frac{\nu}{\mathrm{Pr}}+\varkappa_t\right)\frac{\partial T}{\partial y}\right), \tag{3}$$

$$u\frac{\partial e}{\partial x}+v\frac{\partial e}{\partial y}=\frac{\partial}{\partial y}\left(D\frac{\partial e}{\partial y}\right)+\nu_t\left(\frac{\partial u}{\partial y}\right)^2-\omega, \tag{4}$$

$$u\frac{\partial \lambda}{\partial x}+w\frac{\partial \lambda}{\partial y}=\nu\frac{\partial^2\lambda}{\partial y^2}-0.075\frac{\nu_t\lambda}{e}\left(\frac{\partial u}{\partial y}\right)^2+0.2\left[1-\frac{2\lambda}{y^2}\varphi\left(\frac{2\lambda}{y^2}\right)\right]\frac{\omega L^2}{e}, \tag{5}$$

$$w=v+\frac{\nu}{2\lambda}\frac{\partial\lambda}{\partial y}-\frac{\nu-D}{e}\cdot\frac{\partial e}{\partial y};\quad \varphi(0)=0;\quad \varphi(1)=1. \tag{6}$$

Here u, v, and T are the average velocities and temperature: ν_t and $\varkappa_t$ are the turbulent kinematic viscosity and thermal conductivity; D and ω are the diffusion coefficient and the dissipation of the turbulence energy: $L=\sqrt{2\lambda}$ is the integral scale of turbulence: and e is the specific turbulence energy. The terms on the left-hand side of the transport equations (1)-(5) describe convective transport of the corresponding quantities. The corresponding terms on the right-hand side of (4), (5) describe diffusion of turbulence energy across the layer, energy input from the mean flow, and dissipation of pulsation energy. We point out that the term $w(\partial\lambda/\partial y)$ in the left-hand side of (5) combines the convective $v(\partial\lambda/\partial y)$ and the diffusion terms.

2. Transport Coefficients

The turbulent viscosity and thermal conductivity depend on the quantities e, L, $\partial u/\partial y$, $\partial T/\partial y$, and $\partial e/\partial y$ and are written in the form [5-10]

$$\nu_t=\alpha(z)[1+0.25\xi^2]H\left(\left(\frac{s}{s_1}\right)^2\right)L\sqrt{e};\ \alpha=0.29H\left(\frac{1}{z}\right); \tag{7}$$

$$\varkappa_t=\beta(z)[1+0.25\xi^2]H\left(\left(\frac{s\sqrt{\mathrm{Pr}}}{s_2}\right)^2\right)L\sqrt{e};\ \beta=0.65H\left(\frac{1}{z}\right). \tag{8}$$

A. M. Gor'kii Minsk Pedagogic Institute. Translated from Inzhenerno-Fizicheskii Zhurnal, Vol. 34, No. 6, pp. 1100-1109, June, 1978. Original article submitted June 1, 1977.

0022-0841/78/3406-0745$07.50

Here z and ξ are the dimensionless velocity gradient $z = (L/\sqrt{e})\cdot(\partial u/\partial y)$, and turbulence energy, $\xi = (L/e)\cdot(\partial e/\partial y)$; H is an experimental function of the dimensionless distance to the wall: $s = y\sqrt{e}/\nu$; $s_1 \simeq 30$; $s_2 \simeq 58$,

$$H(t) = \begin{cases} t, & \text{if} \quad t < 0.75, \\ t-(t-0.75)^2, & \text{if} \quad 0.75 \leqslant t \leqslant 1.25, \\ 1, & \text{if} \quad 1.25 < t. \end{cases} \tag{9}$$

The diffusion coefficient of turbulence energy is

$$D = \nu\left(1 + 0.4\frac{L\sqrt{e}}{\nu}H\left(\frac{s}{s_3}\right)\right); \; s_3 \approx 300. \tag{10}$$

The dissipation of turbulence energy is written as follows:

$$\omega = \frac{\nu(1+0.25\xi^2)\,\psi\left(\dfrac{L\sqrt{e}}{\nu}\right)\dfrac{e}{L^2}}{\sqrt{1+2.5\left(\dfrac{\partial L}{\partial y}\right)^2}}. \tag{11}$$

The function $\psi(r)$ takes into account that $\omega \to 5\pi/4$ as $r \to 0$ and $\omega \to 0.4r$ as $r \to \infty$. Thus, $\psi = 0.4r$ for $r > r_1$, while $\psi = 5\pi/4 + br^2$ for $r < r_1$; $b = 0.2/r_1$, $r_1 = 25\pi/4$, $r = L\sqrt{e}/\nu$. Moreover, the function $\varphi(t)$ in (5) can be approximated as follows: $\varphi(t) = 0$ for $0 \le t \le 0.5$ and $\varphi(t) = 4(t - 0.5)^2$ for $0.5 < t \le 1$.

3. Initial and Boundary Conditions

The system (1)-(5) was solved for the following boundary conditions:

$$y = 0;\; u = v = e = L = 0;\; T = T_w. \tag{12}$$

A power-law velocity distribution and a constant temperature were assigned at the exterior limit of the boundary layer:

$$y \to \infty;\; T \to T_\infty;\; e \to e_\infty;\; L \to L_\infty;\; u \to u_\infty;\; u_\infty = cx^m. \tag{13}$$

The intensity and turbulence scale of the outer flow were assigned at the initial point $x(0)$ of the boundary layer [$Re_x(0) = 10^4$]:

$$\frac{u'_\infty(0)}{u_0} = \frac{\sqrt{\frac{2}{3}e_\infty(0)}}{u_0} = 0.025;\; Re_L = \frac{u_0 L_\infty(0)}{\nu} = 500. \tag{14}$$

The energy and turbulence scale of the outer flow vary along x due to dissipation and convection:

$$u_\infty\frac{de_\infty}{dx} = -\omega_\infty;\quad u_\infty\frac{d\lambda_\infty}{dx} = 0.2\frac{\omega_\infty L_\infty^2}{e}. \tag{15}$$

The velocity distribution across the boundary layer at the initial point $x(0)$ in the laminar portion of flow was given for $Re_x = u_\infty(0)x(0)/\nu = 10^4$ in the form $u = u_\infty\Phi'(m, \eta)$, where $\Phi(m, \eta)$ is the self-similar Falkner–Skan solution [1, 2] for $u_\infty = cx^m$. The temperature, energy, and turbulence scale distributions at the point $x(0)$ are similarly given by

$$\theta = \frac{T - T_w}{T_\infty - T_w} = \Phi'(m, \eta\mathrm{Pr}^{\frac{1}{3}});\; e = e_\infty(\Phi')^2;\; L = L_\infty H\left(\frac{y}{\delta}\right). \tag{16}$$

4. Method of Solution and Results

The system of equations (1)-(5) was solved by the finite-difference method, first determining the velocities $u(x + \Delta x, y)$ and $v(x + \Delta x, y)$ from (1) and (2) and then solving the remaining equations. The step Δy varied, since in the viscous sublayer the velocity profiles and those of other parameters vary quickly: $u \sim ay + by^2$; $\theta \sim y$; $L \sim y$; $e \sim y^n$, while in the turbulent part the profiles of all parameters vary slowly: $u \sim a\log y + b$. The calculation showed that in the viscous sublayer there are 5-10 mesh points, while the number of mesh points in y varied with increasing layer thickness from 100 to 350.

Columns 11 and 12 of Table 2 provide the step $\Delta\bar{x}(m)$, corresponding to $\Delta Re_x \simeq Re_x(m + 1)\Delta\bar{x}/\bar{x}$, and the parameter $P = \Delta\bar{x}/\Delta\bar{y}^2_{min}$, by means of which the stability range is usually estimated. It is seen that the step $\Delta\bar{x}$ decreases with decreasing pressure-gradient parameter m. For $\Delta\bar{x}$ = const, the calculation time increases proportionally to Re_x. Increasing the step $\Delta\bar{x}$, to retain the stability it is necessary to increase the step $\Delta\bar{y}_{min}$; in this case it seems that for $Re_x \sim 5.6$ (m = 0) the width of the viscous sublayer becomes smaller than the step of the mesh. This leads to a strong distortion of the velocity profiles and to a loss in stability and accuracy. It is possible that in this case one must replace the velocity profile in the viscous sublayer by its asymptotic value or to choose stretching coordinates taking into account the varying thickness of the viscous sublayer.

In Figs. 1 and 2 we compare results of a numerical calculation of the local resistance coefficient and of the Stanton number for $u_\infty = cx^m$; m = 0; m = 0.1111; m = −0.04762; m = − 0.08676 with theoretical solutions [1, 2] for the laminar portion and with semiempirical dependences [1, 2, 12, 13] for the turbulent portion:

$$c_{f,\,\mathrm{lam}} = \sqrt{2m+2}\,\Phi''(0)\,\mathrm{Re}^{-0.5},\quad \mathrm{St}_{\mathrm{lam}} = K(m,\mathrm{Pr})\,\mathrm{Re}^{-0.5}, \tag{17}$$

$$c_{f,\,\mathrm{turb}} = 0.0592\,\mathrm{Re}^{-0.2},\quad \mathrm{St}_{\mathrm{turb}} = \frac{c_f}{2}\left(\mathrm{Pr} + 0.11\sqrt{\frac{c_f}{2}}\,(\mathrm{Pr}-\mathrm{Pr}_T)\right)^{-1}. \tag{18}$$

The location of the transition point depends on the pressure-gradient parameter m, the intensity $u'(0)/u_0$, the scale $L(0)/x_0$ of the external flow turbulence, and the location of the initial point $Re_x(0)$ in which external turbulence is introduced in the boundary layer, i.e., $Re_{cr} = Re_{cr}[m, \bar{u}'(0), \bar{L}(0), Re_x(0)]$. Table 1 (columns 2, 3, and 4) provides the values of $(\log Re_x)_{cr}$, Re^*_{cr}, Re^{**}_{cr} at the initial point of sharp transition from the laminar to the transition region, i.e., where c_f starts increasing. In column 5 we give the segment length $\Delta Re^* = Re^*_{cr} - Re^*(0)$ from the initial to the transition point. All values in Table 1 are given for various m, but identical values of $\bar{u}'(0)$, $\bar{L}(0)$, and $Re_x(0)$ according to (14). It is seen that the quantity $(Re_x)_{cr}$ increases with increasing m.

Comparing Re^*_{cr} of the transition (column 3) with the theoretical value of Re^*_n at the point of stability loss of laminar self-similar flow (column 6), it is seen that for assigned $\bar{u}'(0)$, $\bar{L}(0)$, and $Re_x(0)$ the transition occurs after the neutral point for m ≤ 0 and earlier than it for m = 0.1111. To realize m = 0.1111 we calculated the variant with external turbulence intensity $\bar{u}'(0) = 0.005$ decreased by a factor of 5. The calculation was extended to $Re_x \simeq 10^7$ ($Re^* \simeq 4000$), i.e., beyond the neutral point ($Re^*_n = 3200$), but the transition point was not reached and the flow remained laminar.

To study the effect of the location of the initial point $Re_x(0)$ for m = 0.1111 and external turbulence parameters (14) we checked the variant with initial point $Re_x(0) = 3\cdot10^4$ instead of $Re_x(0) = 10^4$. It is seen from Figs. 1 and 2 (curves 7) that the further from the edge the plate is, or, stated differently, the closer to the neutral point the external excitation is introduced, the earlier the transition to the turbulent region starts.

At the laminar portion the effect of external flow turbulence begins to practically affect the values of c_f and St at the edge of the portion (particularly for m < 0; Figs. 1 and 2). In the turbulent portion the values of $c_f(m)$ and St(m) increase with increasing m (Figs. 1 and 2), but it is not possible to separate the effects of pressure gradient and of external flow turbulence, since the calculations were performed for the same values of $\bar{e}_\infty(0)$ and $\bar{L}_\infty(0)$.

For all m we calculated the Reynolds similarity parameter $S = 2St/c_f$ and compared it with the theoretical dependences (17), (19), and (20). In Table 2 we provide the relative deviation of the calculated S_C and the theoretical S_T similarity parameter in percents, $\varepsilon = (S_C - S_T)/S_T$. For the laminar portion of the flow the error ε, % is given in column 6 of Table 2 (in the numerator we give ε at the beginning and in the denominator its value at the edge of the laminar portion). The large deviations of S_C from S_T at the beginning of the laminar portion are explained by deviations of the initial temperature profile from the self-similar one, in the middle of the laminar portion the error has decreased to ~5%, and then at the end of the laminar portion (for m = −0.08676), ε increases to 11% due to gradual deviation from the laminar regime (Figs. 1 and 2).

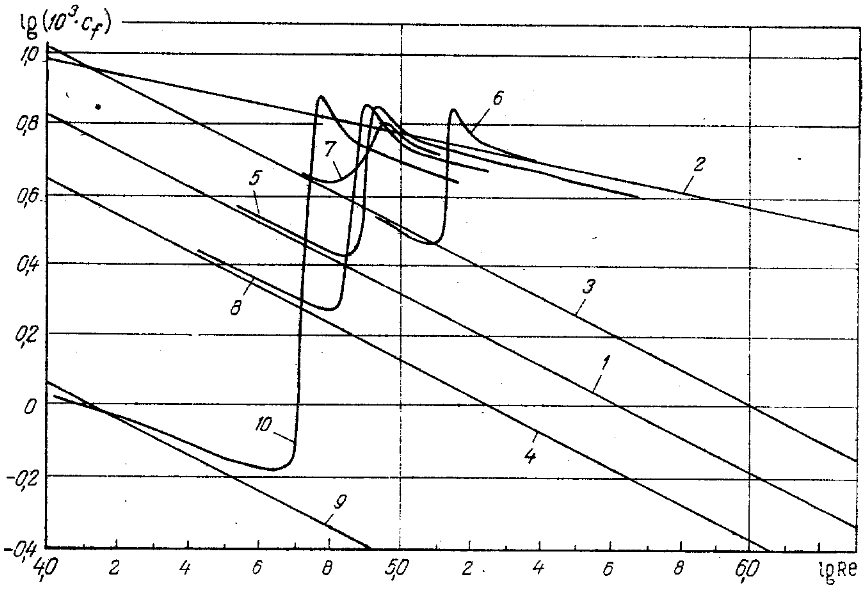

Fig. 1. Local resistance coefficient c_f. Curves 1, 2, 3, 4, and 9 are for dependences of type (17), (18); curves 5, 6, 7, 8, and 10 are calculations for $\overline{u}'_\infty(0) = 0.025$; $Re_L = 500$. Curves 1, 5) m = 0; 3, 6, 7) m = 0.1111; 4, 8) m = −0.04762; 9, 10) m = −0.08676; 5, 6, 8, 10) the initial point Re(0) = 10^4; 7) Re(0) = $3 \cdot 10^4$.

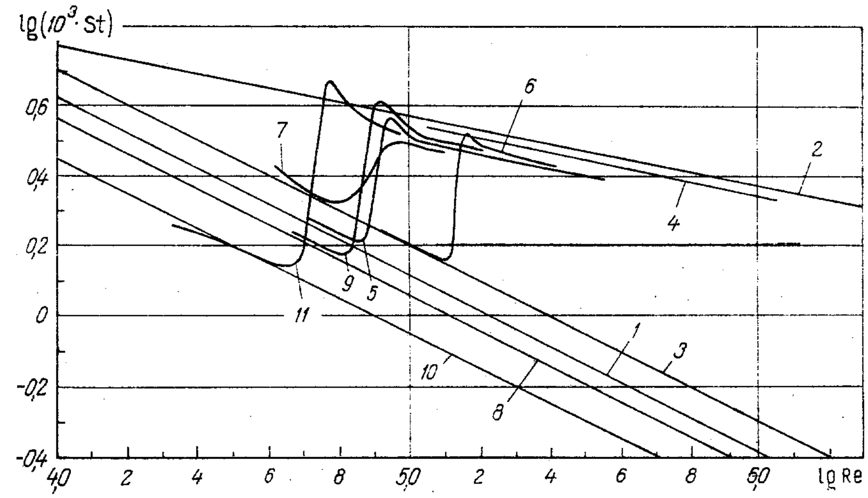

Fig. 2. The local Stanton number St. Curves 1, 2, 3, 4, 8, and 10 are theoretical dependences of type (17), (18); curves 5, 6, 7, 9, and 11 are calculations. Curves 1, 5) m = 0; 3, 6, 7) m = 0.1111; 8, 9) m = −0.04762; 10, 11) m = −0.08676. Curves 5, 6, 9, 11) the initial point Re = 10^4; 7) Re = $3 \cdot 10^4$; 1, 3, 8, 10) $St_{lam} = K(m, Pr)Re^{-0.5}$; 2) $St_T = 0.5c_f Pr^{-2/3}$; 4) $St_T = 0.5c_f[Pr_T + 0.11 \cdot \sqrt{(c_f/2)}\,(Pr - Pr_T)]^{-1}$.

For the turbulent portion the values of ε, % are given in column 7 of Table 2 for Eq. (19) and in column 8 for Eq. (20). The beginning of the turbulent region appears in the numerator of ε and its end appears in the denominator. The following dependences were verified:

$$\frac{c_f}{2St} = Pr \sqrt{\frac{c_f}{2}}\, u_1^+ + \left(1 - u_1^+ \sqrt{\frac{c_f}{2}}\right) + (Pr - 1)\left[A u_1^+ \sqrt{\frac{c_f}{2}} + \frac{Pr - 2}{2} A^2 \frac{c_f}{2} u_1^+\right], \tag{19}$$

$$\frac{c_f}{2St} = Pr \sqrt{\frac{c_f}{2}}\, \delta_1^+ + Pr_T \left(\frac{\tau_1}{\tau_w}\right)\left(1 - u_1^+ \sqrt{\frac{c_f}{2}}\right) +$$

TABLE 1. Parameter Values at the Transition Point (columns 2-6) and the Ratio of u_p^+ to the Theoretical Value (columns 7-11)

1	2	3	4	5	6	7	8	9	10	11	12
m	$(\lg Re_x)_{cr}$	Re^*_{cr}	Re^{**}_{cr}	ΔRe^*_{cr}	Re^*_n	$\lg Re_x$	Re^*	Re^{**}	Φ	$\frac{u_p^+ - u_T^+}{u_T^+}$	$\frac{\alpha}{\lg a}$
−0,08676	4,65	604	178	303	—	4,86	454	280	0,923	$\frac{6}{9}$	$\frac{9,03}{-40,8}$
−0,04762	4,81	507	187	291	126	5,007	486	301	0,416	$\frac{6}{6}$	$\frac{6,91}{-31,54}$
0	4,85	433	174	261	420	5,004	400	324	0	$\frac{5}{4}$	$\frac{5,89}{-26,76}$
0,11111	5,09	454	195	320	3200	5,266	508	318	−0,58	$\frac{-3}{-2}$	$\frac{8,91}{-43,46}$

TABLE 2. Parameters of Calculating the Turbulent Portion [columns 2 and 3 are log Re_x and Re^{**} for max c_f; 4 and 5 are the limits of this range in log Re_x and Re^{**}; 9 and 10 are the ratios δ/Δ and τ_1/τ_w; the numerator is the initial value and the denominator is the edge of the turbulent region (columns 4-8]

1	2	3	4	5	6	7	8	9	10	11	12
m	$\lg Re_x$	Re^{**}	$\lg Re_x$	Re^{**}	ε_{lam}, %	ε_{turb}, %	ε_{turb}, %	$\frac{\delta}{\Delta}$	$\frac{\tau_1}{\tau_w}$	$\Delta\bar{x}$	P
−0,08676	4,77	230	$\frac{4,799}{5,101}$	$\frac{234}{465}$	$\frac{-20}{-11}$	$\frac{+1}{+6}$	$\frac{-1}{+4}$	$\frac{1,01}{1,01}$	$\frac{1,07}{1,06}$	$0,33\cdot10^{-4}$	0,3
−0,04762	4,91	230	$\frac{4,984}{5,254}$	$\frac{285}{535}$	$\frac{-7}{-3}$	$\frac{-4}{+2}$	$\frac{-6}{+2}$	$\frac{0,9}{0,92}$	$\frac{1,03}{1,02}$	$0,13\cdot10^{-3}$	0,6
0	4,94	210	$\frac{5,099}{5,638}$	$\frac{325}{1002}$	$\frac{-2}{-6}$	$\frac{-5}{+4}$	$\frac{-5}{+4}$	$\frac{0,83}{0,85}$	$\frac{1}{1}$	$0,1\cdot10^{-3}$	0,6
+0,1111	5,15	223	$\frac{5,191}{5,433}$	$\frac{219}{470}$	$\frac{+23}{+4}$	$\frac{-16}{-8}$	$\frac{-9}{-6}$	$\frac{0,7}{0,74}$	$\frac{0,95}{0,96}$	$0,13\cdot10^{-3}$	0,6

$$+\frac{\Pr_T}{k}\sqrt{\frac{\tau_1}{\tau_w}}\sqrt{\frac{c_f}{2}}\left[\ln\frac{\Delta}{\delta}+\ln\frac{\delta_1}{\delta_2}+\ln\frac{a_2}{a_1}\right]. \tag{20}$$

Here $A = -\rho\mu u_\infty(du_\infty/dx)/\tau_w^2$; $a_i = 1 + (k\Pr/\Pr_t)\sqrt{(\tau_1/\tau_w)}\,\delta_i^+$; $i = 1,2$; $k = 0.4$.

Equation (19), derived [12] for $\Pr_T = 1$ and linear dependence of $\tau(u)$ in the viscous sublayer, gives fairly good agreement with the calculations, except for the variant with negative pressure gradient ($m = 0.1111$). Estimates show that in this case the thicknesses δ and Δ of the turbulent dynamic and thermal layers (column 9, Table 2) differ strongly. This is why Eq. (20), explicitly taking into account the difference between the thicknesses Δ and δ of the thermal and dynamic layers and the difference between the thicknesses δ_1 and δ_2 of the viscous dynamic and thermal sublayers, was suggested. In deriving (20, we applied the two-layer scheme for the velocity $0 < \delta_1 < \delta$, and the three-layer scheme for temperature $0 < \delta_1 < \delta_2 < \Delta$:

$$u^+ = y^+ + A_1(y^+)^2;\ T^+ = T_w^+ + u^+\Pr;\ y < \delta_1;\ A_1 = \frac{\nu}{2\rho u_*^3}\cdot\frac{dp}{dx}; \tag{21}$$

$$u^+ = u_\infty^+ + \frac{1}{k}\sqrt{\frac{\tau_1}{\tau_w}}\ln\left(\frac{y}{\delta}\right);\ \delta_1 \leqslant y \leqslant \delta;\ \frac{\tau_1}{\tau_w} = 1 + 2A_1\delta_1^+; \tag{22}$$

$$T^+ = T_2^+ + \frac{1}{k}\Pr_T\sqrt{\frac{\tau_1}{\tau_w}}\ln\left(\frac{1+\frac{k\Pr}{\Pr_T}\sqrt{\frac{\tau_1}{\tau_w}}\,y^+}{1+\frac{k\Pr}{\Pr_T}\sqrt{\frac{\tau_1}{\tau_w}}\,\delta_2^+}\right);\ \delta_1 \leqslant y \leqslant \delta_2; \tag{23}$$

$$T^+ = T_\infty^+ + \frac{\Pr_T}{k}\sqrt{\frac{\tau_1}{\tau_w}}\ln\left(\frac{y}{\delta}\right);\ \delta_2 < y \leqslant \Delta. \tag{24}$$

Here $T^+ = T/T_*$; $u^+ = u/u_*$; $T_* = q_w/\rho c_p u_*$; $u_* = \sqrt{\tau_w/\rho}$; $\tau_1 = \tau_w + (dp/dx)\delta_1$ is the friction at the boundary of the viscous sublayer of thickness δ_1. To include the effect of pressure gradient on the thickness of the viscous sublayer δ_1, it was suggested [14] that $(\delta_1/\nu)\cdot\sqrt{\tau_1/\rho} = \alpha$ for $\alpha = 11.6$. Equation (20) is valid for $\delta_1 \leq \delta_2$, and putting $\delta = \Delta$, $\delta_1 = \delta_2$, $\tau_1 = \tau_w$, and $dp/dx = 0$ in (20), the well-known behavior of the Reynolds similarity parameter [1, 2] is obtained.

Figures 3 and 4 show the dimensionless velocity and temperature profiles compared with semiempirical dependences for a viscous sublayer and logarithmic portion:

$$u^+ = 5.6\lg y^+ + 4.9;\quad u^+ = 5.75\lg y^+ + 5.5; \tag{25}$$

$$\theta^+ = 4.7\lg y^+ + 4.6;\quad \delta_1^+ = u_1^+ = \alpha;\quad \alpha = 11.6. \tag{26}$$

Here the experimental dependence of θ^+ is taken from [11] for $u_\infty'/u_0 \simeq 0.02$. Generally, for $dp/dx \neq 0$ it is better to replace (25) by (27), which was derived similarly to (25), but taking into account the effect of a pressure gradient:

$$u^+ = \frac{1}{k}\sqrt{\frac{\tau_1}{\tau_w}}\ln y^+ + \left(u_1^+ - \frac{1}{k}\sqrt{\frac{\tau_1}{\tau_w}}\ln\delta_1^+\right);\ \delta_1^+ = \alpha\sqrt{\frac{\tau_w}{\tau_1}}. \tag{27}$$

Here $\alpha = 11.6$; $k = 0.4$; $\tau_1/\tau_w = 1 + 2A_1\delta_1^+$; $A_1 = (\nu/2\rho u^3)\cdot(dp/dx)$; $\tau_1 = \tau_w + (dp/dx)\delta_1$ is the friction at the boundary of the viscous sublayer. If $dp/dx = 0$, (27) coincides with (25). It is seen from (27) that for $dp/dx \neq 0$ ($\tau_1 \neq \tau_w$) the slope of u^+ in the coordinates $\ln y^+$ is changed by a factor $\sqrt{\tau_1/\tau_w}$ and, similarly, δ_1^+ is changed by $\sqrt{\tau_1/\tau_w}$ times. Thus, for $dp/dx > 0$ ($\tau_1 > \tau_w$) the thickness of the viscous sublayer δ_1^+ decreases with respect to the nongradient flow, while for $dp/dx < 0$ it increases. The slope of u^+ decreases for $dp/dx < 0$ and increases for $dp/dx > 0$.

In Table 1 (columns 7-11) we compare the calculated profiles of $u_C^+(y^+)$ with the theoretical $u_T^+(y^+)$ taken from (27) in the region $1.3 < \log y^+ < 1.9$, i.e., in the region of the "wall law" [1, 2]. Column 11 gives the relative deviation $(u_C^+ - u_T^+)/u_T^+$ in percent, with the numerator containing the error for $\log y^+ = 1.3$ and the denominator containing the same quantity for 1.9.

Columns 7-10 provides the values of Re_x, Re^*, Re^{**}, and $\Phi = (\delta/\tau_w)\cdot(dp/dx)$, for which the profiles $u_C^+(y^+)$ were calculated. It is seen that the agreement of the calculated values

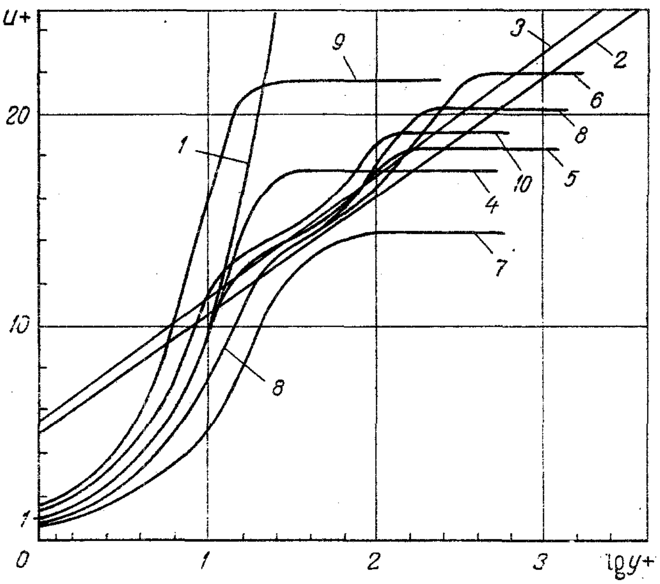

Fig. 3. Dimensionless velocity profiles $u^+(y^+)$. Curves 1, 2, and 3 are theoretical dependences; curves 4, 5, 6, 7, 8, 9, and 10 are calculations. Curve 1) $u^+ = y^+$; 2) $u^+ = 5.6 \cdot \log y^+ + 4.9$; 3) $u^+ = 5.75 \log y^+ + 5.5$; 1, 2, 3, 4, 5, 6) m = 0; 7, 8) m = 0.1111; 9, 10) m = −0.04762; 4, 7, 9) Re = 10^4; 5, 10) Re = 10^5; 6) Re = $4 \cdot 10^5$; 8) Re = $2 \cdot 10^5$.

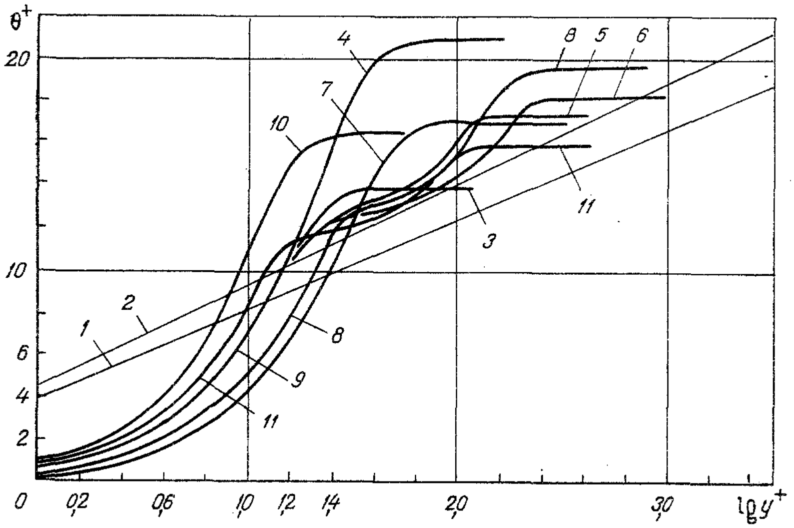

Fig. 4. Dimensionless temperature profiles $\theta^+(y^+)$. Curve 1) $\theta^+ = 4.2 \log y^+ + 3.9$; 2) $\theta^+ = 4.7 \log y^+ + 4.6$; 9) $\theta^+ = y^+ \mathrm{Pr}$. Curves 3, 4-8, 10, 11) calculations; 1, 2-6) m = 0; 7, 8) m = 0.1111; 10, 11) m = −0.04762; 3, 10) Re = 10^4; 4, 7) Re = $4 \cdot 10^4$; 5, 11) Re = 10^5; 8) Re = $2 \cdot 10^5$; 6) Re = $4 \cdot 10^5$.

$u_c^+(y^+)$ with (27) is quite good. Thus, the pressure gradient affects the velocity profile in the whole layer, and the velocity profiles are stratified in such a manner that in the region of the "wall law" $u^+(y^+, A_1') \neq u^+(y^+, A_1'')$ if $A_1' \neq A_1''$, $A_1 = (\nu/2\rho u^3) \cdot (dp/dx)$. In the external part of the layer $u^+ \to \sqrt{2/C_f}$ for $y^+ \to \infty$, i.e., it also depends on dp/dx.

In the transition region log Nu_x depends linearly on log Re_x. This allows one to approximate results of calculating Nu_x in the transition region for assigned m in the form of a power law: $Nu_x = a Re^{\alpha}$. The coefficients a and α depend on m and are given in Table 1 (column 12, with α in the numerator and log a in the denominator).

As a whole, the results of calculations for $u_\infty = cx^m$ imply good qualitative agreement between the flow model treated here and semiempirical theories and experiments [1, 2, 12, 13].

At the same time, this model enables one to take into account effectively real external parameters affecting the flow in a boundary layer, such as the intensity and scale of turbulence of a leaking flow, as well as to simultaneously perform calculations in the laminar, turbulent, and transition regions of the flow.

NOTATION

$e = 0.5\Sigma\overline{u_i'u_i'}$, specific turbulence energy; c_f, local resistance coefficient; St = Nu/Pe, local Stanton number; $u^+ = u/u_*$, $y^+ = yu_*\nu^{-1}$, dimensionless velocity and distance; $u_* = u_\infty\sqrt{0.5c_f}$; $t_* = q_w(\rho c_p u_*)^{-1}$, dynamic velocity and temperature; $\theta = (T - T_w)t^{-1}$, dimensionless temperature; Re*, Re**, Reynolds numbers with characteristic dimensions δ^* and δ^{**}; m, exponent in expression for velocity of external flow $u_\infty = cx^m$; $\beta = 2m(m+1)^{-1}$, parameter of self-similar solutions; τ_1, friction at the boundary of the viscous sublayer; u_1, δ_1, velocity and thickness of the viscous sublayer; δ_2, thickness of the thermal sublayer; δ, Δ, thickness of the dynamic and thermal turbulent layers.

LITERATURE CITED

1. L. G. Loitsyanskii, Mechanics of Liquids and Gases [in Russian], Nauka, Moscow (1973).
2. H. Schlichting, Boundary Layer Theory, 6th ed., McGraw-Hill, New York (1968).
3. A. N. Kolmogorov, Dokl. Akad. Nauk SSSR, 30, No. 4 (1941).
4. I. Rotta, Z. Phys., 129, No. 6 (1951).
5. G. S. Glushko, Izv. Akad. Nauk SSSR, Mekh., No. 4 (1965).
6. G. S. Glushko, in: Turbulent Flows [in Russian], Nauka, Moscow (1970).
7. G. S. Glushko, Izv. Akad. Nauk SSSR, Mekh. Zhidk. Gaza, No. 4 (1971).
8. G. S. Glushko, Izv. Akad. Nauk SSSR, Mekh. Zhidk. Gaza, No. 3 (1972).
9. G. S. Glushko and V. A. Solopov, Izv. Akad. Nauk SSSR, Mekh. Zhidk. Gaza, No. 4 (1972).
10. V. A. Solopov, Izv. Akad. Nauk SSSR, Mekh. Zhidk. Gaza. No. 5 (1972).
11. A. A. Shlanchyauskas and M. R. Drizhyus, Tr. Akad. Nauk LitSSR, Ser. B, 1 (1971).
12. I. P. Ginzburg, Theory of Resistance and Heat Transfer [in Russian], Izd. LGU, Leningrad (1970).
13. K. K. Fedyaevskii, A. S. Ginevskii, and A. V. Kolesnikov, Calculation of Turbulent Boundary Layers of Incompressible Liquids [in Russian], Sudostroenie, Leningrad (1973).
14. S. S. Kutateladze and A. I. Leont'ev, Turbulent Boundary Layers of a Compressible Gas [in Russian], Izd. Sibirsk. Otd. Akad. Nauk SSSR, Novosibirsk (1962).